American Journal of Astronomy and Astrophysics
2024, Vol. 11, No. 2, pp. 51-64
https://doi.org/10.11648/j.ajaa.20241102.12

Research Article

An Analytical Model for Cosmology with a Single Input, the Redshift

Naser Mostaghel*

Department of Civil Engineering, University of Toledo, Toledo, USA

Abstract

We propose an analytical model for cosmology which requires only one parameter as an input. This parameter is the redshift. The model is based on conservation of energy, Planck's Radiation Law, and the relation between energy and frequency of waves. The model yields the current age of the universe, the age of the universe at the CMB emission, as well as the time histories of its expansion velocity and acceleration. The model also is used to show the existence of a constant energy per unit area, associated with the momentum energy of photons, which generates the pressure that perpetuates the expansion of the universe. The model is completely independent of the ΛCDM model but implicitly includes the effects of gravity. Using the model we show the existence of a constant in nature that under certain assumptions can represent the Hubble constant. We have used the model to derive the Hubble constants measured by Reiss et al. and by the Planck Collaboration. Using the model we show that the path of light in the Planck collaboration measurement is along a circular arc, while the Reiss et al. measurement path is exactly along the chord of the same circular arc. The difference in the light travel times along these two paths matches exactly the difference between the two measured values for the Hubble constant, as measured by Reiss et al. and as measured by the Planck Collaboration. This result explains the cause of tension between the two methods of measurement.

Keywords

Cosmology: Theory, Galaxies: High-Redshift, Galaxies: Distances and Redshift

1. Introduction

The only observable and measurable parameter in observational cosmology is the redshift. But the current ΛCDM cosmological model, involves, besides the measured redshift, z, additional derived parameters, such as the Hubble constant, H_0, and the density parameter, Ω_m. Reiss et al. [1], using the cosmic distance ladder approach, have reported values for the Hubble constant of the order of $H_0 = 73.2 \pm 1.3\ \mathrm{km\ s^{-1}Mpc^{-1}}$. But the Planck Collaboration ΛCDM fit to the Planck observations, using CMB temperature fluctuations power spectra, has reported values of the order of $H_0 = 67.4 \pm 0.5\ \mathrm{km\ s^{-1}Mpc^{-1}}$, Aghanim et al. [2]. There are significant differences in these reported values of H_0. However, in spite of continuing investigations, Di Valentino, et al. [3, 4], Abbott, et al. [5], Schombert, et al. [6], Freedman, et al. [7], Huang, et al. [8], Bull, et al. [9], and improvements in the measurement methodology and precision, it has not been possible to explain the cause of the tension in the measurements of H_0 via the standard ΛCDM model. The Boylan-Kolchin and Weisz [10] investigation also shows that in the modified model, Early Dark Energy (EDE),

*Corresponding author: naser.mostaghel@utoledo.edu (Naser Mostaghel)

Received: 1 June 2024; **Accepted:** 25 June 2024; **Published:** 8 July 2024

the redshift-time relation is in tension with that of ΛCDM. Also the ΛCDM model suffers from the elusive nature of its Cold Dark Matter (CDM). Multiple ground based searches for a Weakly Interactive Massive Particle (WIMP) have found no convincing evidence of dark matter, Jakobsen, et al. [11], Roszkowski, et al. [12]. Also there are stars and other celestial bodies whose redshift, based on the Planck cosmology, suggests their formation before the era of reionization, Schlaufman, et al. [13], Hill, et al. [14]. As there has been no satisfactory resolution of the tension, there are discussions of needs for possibly new physics, Abdalla, et al. [15], Greene and Perlmutter [16], Freedman [17], Pasten, et al [18]. The new James Webb Space Telescope (JWST) with its Near-Infrared Spectrograph provides opportunities for detection and characterization of high redshift early galaxies which can provide constraints and be used to test the predictions and reliability of various models, Robertson, et al. [19], Curtis-Lake, et al. [20], Brinchmann [21].

Boylan-Kolchin and Weisz consider the discrepancy in the reported values of H_0 to be due to issues of precision and accuracy and the possibility of incompleteness of the ΛCDM model. Consistent values for quantities such as the age of the universe, the age of the universe at CMB emission, and the relation between redshift and look-back-time are necessary for understanding the conditions of formations of early galaxies and other structures. The standard ΛCDM model has been successful in addressing many cosmological problems. However, the persistence of the Hubble tension and the elusiveness of dark matter/energy have given rise to major issues. Here we present a model that is totally independent of the ΛCDM model. It involves neither the Hubble constant nor dark matter/energy. There is no derived parameter in this model; the only necessary input to the model is the redshift, whether measured or assumed. The model is based on the conservation of energy and the assumption of isotropy. It implicitly includes the effects of gravity, as described by General Relativity. The model yields the relationship between redshift and the look-back-time, and it predicts the age of the early dark universe when waves start to be emitted, the age of the visible universe, the age of the universe at the CMB emission, and the maximum range of visibility in the future. It also yields the variations of the expansion velocity and expansion acceleration with look-back-time. In addition the model predicts that it is a constant surface energy density equal to $\rho_A = 5.95472 \times 10^{19}\ \mathrm{j.m^{-2}}$ that perpetuates the expansion of the universe. Finally the model is used to evaluate the Hubble constant, H_0, and show the cause of tension in its measurements.

The evaluations of the energy of radiated photons and the energy of emitted waves are discussed in sections 2 and 3. Age evaluation, relation between look-back-time and redshift, and the model's predictions are presented in sections 4, 5 and 6. Consistency of the model's predictions with observational data, the cause of tension in the measurements of the Hubble constant, together with summary and conclusions are presented in sections 7, 8 and 9.

2. Evaluation of Total Energy of Scattered Photons Using Planck's Radiation Law

Almost all our knowledge about the cosmos is based on the properties of light rays encapsulated in the measured or assumed value of redshift. To use the conservation of energy law, we will first use Planck's radiation law to calculate the total energy radiated as photons from the surface of last scattering. Spectral radiance represents power per steradian per cubic meter. It is defined by Planck's Law, Goldin [22], Kramm and Molders [23] as

$$B(\lambda, T) = \frac{2hc^2}{\lambda^5}\left(e^{\frac{hc}{\lambda kT}-1}\right)^{-1}, \quad (1)$$

where c is the speed of light, $h = 6.62607 \times 10^{-34}\ \mathrm{J\,K^{-1}}$ is the Planck constant, k is the Boltzmann constant, T represents the temperature at the recombination era, and λ represents the wavelength. Integrating the spectral radiance as defined in equation (1) over the wavelength from $\lambda = \lambda_P$ to various values of λ from $\lambda = 10^{-3}\ \mathrm{m}$ to $\lambda = 10^{10}\ \mathrm{m}$ shows that the value of U does not change, and it is given by

$$U = \int_{\lambda_P}^{10^{-3}} \frac{2hc^2}{\lambda^5}\left(e^{\frac{hc}{\lambda kT}} - 1\right)^{-1} d\lambda \approx \int_{\lambda_P}^{10^{10}} \frac{2hc^2}{\lambda^5}\left(e^{\frac{hc}{\lambda kT}} - 1\right)^{-1} d\lambda \approx 1.46199639 \times 10^6\ \mathrm{W.sr^{-1}.m^{-2}}. \quad (2)$$

In the above relation the wavelength, λ_P, is represented by the Planck length, that is, $\lambda_P = 1.61623 \times 10^{-35}\ \mathrm{m}$, and U represents power per steradian per unit area of the surface of last scattering. Equation (2) shows that the calculated value for U is essentially a constant. To calculate the total energy emitted by the released photons, we need to calculate the total area of the surface of last scattering.

According to the cosmological redshift paradigm, Simionato [24], the expansion of space increases the distance among the celestial bodies. As a result of the cosmic expansion, the light waves are stretched. The ratio of the emitted wave length, λ_{emi}, and the observed wave length, λ_{obs}, is expressed by

$$\frac{\lambda_{obs}}{\lambda_{emi}} = \frac{R(t_{obs})}{R(t_{emi})} = 1 + z = \frac{c\,t_{obs}}{c\,t_{emi}} = \frac{t_{obs}}{t_{emi}}, \quad (3)$$

where c represents the speed of light and R represents the scale factor. Let t_{emi} represent the time when electromagnetic waves start to be emitted. Due to the expansion of the universe the wave lengths of these waves stretch by the factor $(1 + z_s)$ as they reach to the surface of last scattering. The surface of last scattering at which the photons are released is associated with the universe having cooled down, due to its expansion, to a temperature of about 3000 K, corresponding to the redshift $z_s = z_{CMB} \cong 1090$ associated

with the surface of last scattering Fixsen [25]. As the result of the expansion, the radius of the surface of last ing, r_s is given by

$$r_s = c\,(1 + z_s)\,t_{emi} = c\,t_{obs}. \quad (4)$$

Equation (4) is for a specific value of $z = z_s = 1090$. For values of redshift $0 \le z \le z_s$ and $> t_{emi}$, equation (4) is replaced by

$$r = c\,(1 + z)t_{emi} = c\,t, \quad (5)$$

The above relation implies that during any time interval space expands by the factor $(1 + z)$, where z represents the redshift. Considering equations (2) and (4), the total energy, E_1, released at the surface of last scattering by the photons at the redshift $z = z_s = 1090$ is given by

$$E_1 = U(\lambda, T)\,(4\pi\,{r_s}^2)\,\pi\,t_{emi} = U(\lambda, T)\,4\pi^2c^2(1 + z_s)^2\,{t_{emi}}^3. \quad (6)$$

3. Evaluation of the Total Energy of Emitted Waves

We calculate the total input energy using Planck's relation between energy and frequency of the waves. The total input energy is supplied by the energy of the waves emitted at the "big bang." To calculate the input energy, we assume that the shortest wavelength, λ_e, of waves emitted at the "big bang" is equal to the Planck length, that is $\lambda_e = \lambda_P = 1.61623 \times 10^{-35}$ m. Thus the corresponding "observed" wavelength, λ_o, is given by

$$\lambda_o = (1 + z_s)\,\lambda_e = (1 + z_s)\,\lambda_P. \quad (7)$$

The number of "observed" waves, n_o, and the number of emitted waves, n_e, are calculated as follows:

$$n_o = \frac{c\,t_o}{2\,\lambda_o} = \frac{c\,t_{obs}}{2\,(1+z_s)\,\lambda_P}, \quad (8)$$

$$n_e = \frac{c\,t_{obs}}{2\,\lambda_P} \quad (9)$$

and the wavelength of the n^{th} wave is defined by

$$\lambda_n = \frac{c\,t_{obs}}{n}, \quad (10)$$

which yields the period of the n^{th} wave, p_n, as

$$p_n = \frac{\lambda_n}{c} = \frac{t_{obs}}{n}, \quad (11)$$

where t_{obs} represents the temporal radius of the surface of last scattering. Considering each wave to be associated with an oscillator, according to Planck, each oscillator can absorb or emit a quantum of energy given by

$$\Delta E_n = \frac{h}{p_n} = n\,\frac{h}{t_{obs}}. \quad (12)$$

Thus the total energy emitted by all these oscillators is given by

$$E_2 = \sum_{n_o}^{n_e} \Delta E_n = \sum_{n_o}^{n_e} n\,\frac{h}{t_{obs}} = \frac{h}{t_{obs}} \sum_{n_o}^{n_e} n = \frac{h}{t_{obs}} \sum_{\frac{c\,t_{obs}}{2\,(1+z_s)\,\lambda_P}}^{\frac{c\,t_{obs}}{2\,\lambda_P}} n. \quad (13)$$

4. Age Evaluations

In this section we present the details of the evaluation of the age of the early dark universe, the age of the universe at the CMB emission as evaluated at the present time, the age of the visible universe at the present time, and the maximum range of visibility in the future.

4.1. Evaluation of the Age of the Visible Universe at the Present Time

At the time $t = t_{obs}$ and $z = z_s = 1090$, considering the principle of conservation of energy, we equate the total output energy, E_1, from equation (6) to the total input energy, E_2, from equation (13). This equality of total input and total output energies yields the following cubic equation for t_{emi}.

$$U(\lambda, T)\,4\pi^2c^2(1 + z_s)^2\,{t_{emi}}^3 = \frac{h}{t_{obs}} \sum_{\frac{c\,t_{obs}}{2\,(1+z_s)\,\lambda_P}}^{\frac{c\,t_{obs}}{2\,\lambda_P}} n. \quad (14)$$

The above cubic equation has three roots with the same magnitudes. The magnitude of the root is given by

$$t_{emi} = \left(\frac{\frac{h}{t_{obs}} \sum_{\frac{c\,t_{obs}}{2\,(1+z_s)\,\lambda_P}}^{\frac{c\,t_{obs}}{2\,\lambda_P}} n}{U(\lambda,T)\,4\pi^2c^2(1+z_s)^2} \right)^{1/3}. \quad (15)$$

This equation involves two unknowns: the time t_{emi}, and the time t_{obs}. But, based on equation (4),

$$t_{obs} = \left(\frac{1+z_s}{2}\right) t_{emi}. \quad (16)$$

The $\frac{1}{2}$ factor in the above equation accounts for the fact that the redshift z_s is associated with space, but the flow of time is isotropic. Now substitution for t_{emi} from equation (15) into the above equation yields.

$$t_{obs} = \left(\frac{1+z_s}{2}\right) \left(\frac{\frac{h}{t_{obs}} \sum_{\frac{c\,t_{obs}}{2\,(1+z_s)\,\lambda_P}}^{\frac{c\,t_{obs}}{2\,\lambda_P}} n}{U(\lambda,T)\,4\pi^2c^2(1+z_s)^2} \right)^{1/3}. \quad (17)$$

The only unknown in this equation is t_{obs}. The solution of the above equation yields the value of t_{obs} as

$$t_{obs} = 8.65555 \times 10^{14}\ s = 2.74278 \times 10^{7} y. \quad (18)$$

t_{obs} in the above equation represents the temporal radius of the surface of last scattering. Substitution of t_{obs} from the above equation back into equation (15) yields the value of the time t_{emi} as

$$t_{emi} = \left(\frac{\frac{h}{t_{obs}} \sum^{\frac{c\, t_{obs}}{2\, \lambda_P}} n}{U(\lambda,T)\, 4\pi^2 c^2 (1+z_s)^2} \right)^{1/3} = \frac{t_{obs}}{(1+z_s)/2} = 50280.1\ y. \quad (19)$$

It should be noted that this age is associated with the time when the waves start to be emitted. The time t_{emi} can be considered to be the temporal radius of the early dark universe. The emitted waves are "observed" at the time t_{obs}, as given by equation (18). Between the time t_{emi} and t_{obs} the universe is still dark. The time t_{obs} is when the photons are released, that is, when they become transparent. This time is associated with the universe having cooled down to a temperature of about 3000 K, corresponding to the redshift $z = z_s = z_{CMB} \cong 1090$.

To calculate the age of the universe at the present time, we note that during the time interval from the big bang till the time t_{obs}, given in equation (18), due to the expansion of space, the temporal radius of the universe has increased by the factor $\left(\frac{1+z_s}{2}\right)$. Therefore, using equations (17) and (18), the present age of the visible universe, t_0, is given by

$$t_0 = \left(\frac{1+z_s}{2}\right) t_{obs} = \left(\frac{1+z_s}{2}\right) 8.65555 \times 10^{14}\ s = 4.7216 \times 10^{17}\ s = 14.96185\ Gy. \quad (20)$$

Substitution of $t_0 = 14.96185$ Gy for t_{obs} in equation (15) yields the age of the CMB emission, evaluated at the present time when the universe has cooled down to a temperature of $T_0 = 2.752799$ K, as

$$t_{CMB} = \frac{1}{y} \left(\frac{\frac{h}{t_0} \sum^{\frac{c\, t_0}{2\, \lambda_P}} n}{U(\lambda,T)\, 4\pi^2 c^2 (1+z_s)^2} \right)^{1/3} = 410{,}828.598693\ y. \quad (21)$$

Using the following Schwarzschild relation [26], one obtains t_{CMB} as

$$t_{CMB} = \frac{t_0}{1+(1+z_s)^{3/2}} = \frac{14.961853\ Gy}{1+(1+1090)^{3/2}} = 415{,}180\ y \quad (22)$$

which differs by less than 1.1% from the value given by equation (21).

For values of redshift $0 \le z \le z_s$, we find the relation between the time and redshift via equations (5) and (17). In light of equation (5), we replace the redshift term z_s by z in equation (17). Note that the constant term $\left(\frac{1+z_s}{2}\right)$ does not change. Also, we replace the term t_{obs} on the right hand side of equation (17) by the present time age of the visible universe, t_0. This process yields the relation between the cosmic time, $\bar{t}_c$, and the redshift as

$$\bar{t}_c = \left(\frac{1+z_s}{2}\right) \left(\frac{\frac{h}{t_0} \sum^{\frac{c\, t_0}{2\, \lambda_P}} n}{U(\lambda,T)\, 4\pi^2 c^2 (1+z)^2} \right)^{1/3}. \quad (23)$$

A plot of the above equation for $0 \le z \le 20$ is presented in figure 1.

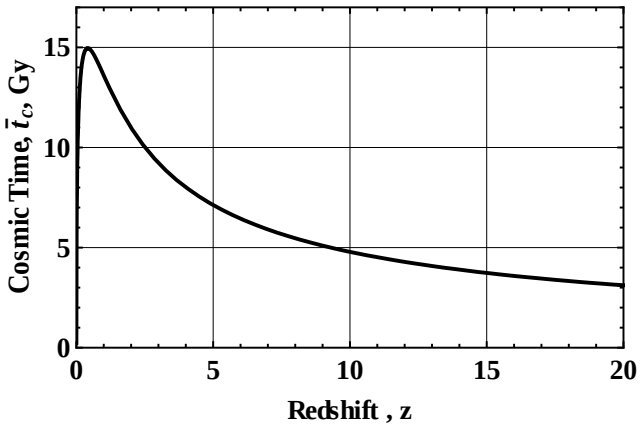

Figure 1. *Variations of the Cosmic Time with Redshift.*

The maximum value of the cosmic time in this figure appears to match the present-time value of the age of the visible universe as given by equation (20). However, the position of the maximum is away from $z = 0$ by an unknown amount, z_0. We find the value of z_0 through differentiating equation (23) with respect to z and setting the resulting derivative equal to zero. This process yields

$$z_0 = \sqrt{2.0} - 1.0. \quad (24)$$

The maximum value of the cosmic age of the observable universe should occur at redshift equal to zero. Its shift from $z = 0$ to $z_0 = \sqrt{2.0} - 1.0$, is due to an increased number of waves that should be included in the expression for the input energy. Replacing the redshift, z, in the numerator of equation (23) by $z = z + z_0$ increases the number of the waves and transforms equation (23). As the result of this transformation the cosmic time, t_c, is given by

$$t_c = \left(\frac{1+z_s}{2}\right)\left(\frac{\frac{h}{t_0}\sum^{\frac{c\,t_0}{2\,\lambda_P}}\left(\frac{c\,t_0}{2\,(1+z+z_0)\lambda_P}\right)^n}{U(\lambda,T)\,4\pi^2c^2(1+z)^2}\right)^{1/3}. \quad (25)$$

A plot of the above equation for $0 \le z \le 20$ is presented in figure 2.

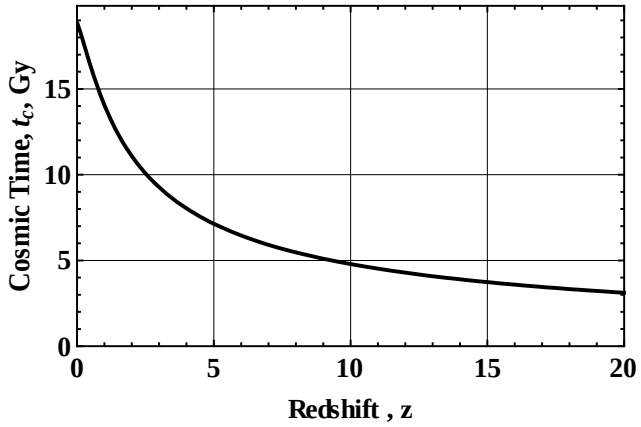

Figure 2. *Variations of the Cosmic Time with Redshift.*

Equation (25) yields the value of t_c for the redshift $z = z_s$, at the present time as

$$\Delta t_c = \left(\frac{1+z_s}{2}\right)\left(\frac{\frac{h}{t_0}\sum^{\frac{c\,t_0}{2\,\lambda_P}}\left(\frac{c\,t_0}{2\,(1+z_s+z_0)\lambda_P}\right)^n}{U(\lambda,T)\,4\pi^2c^2(1+z_s)^2}\right)^{1/3} = 0.224107\ \text{Gy}. \quad (26)$$

In the above equation Δt_c represents the temporal radius of the surface of last scattering at the present time. Because the value of Δt_c occurs at $z = z_s = 1090$, it sets the limit on how close we can get to the instant of the big bang.

Setting the redshift, z, in equation (25) to zero yields the maximum value of the cosmic time t_c as

$$t_{cMax} = \left(\frac{1+z_s}{2}\right)\left(\frac{\frac{h}{t_0}\sum^{\frac{c\,t_0}{2\,\lambda_P}}\left(\frac{c\,t_0}{2\,(1+z_0)\lambda_P}\right)^n}{U(\lambda,T)\,4\pi^2c^2}\right)^{1/3} = 18.850753\ \text{Gy}. \quad (27)$$

It will be shown that t_{cMax} represents the future maximum range of visibility.

4.2. Evaluation of the Relation of the Look-Back Time and Redshift

The relation between the look-back-time, t_{LB}, and redshift is given by

$$t_{LB} = t_{cMax} - t_c = 18.850753\ \text{Gy} - \frac{1}{\text{Gy}}\left(\frac{1+z_s}{2}\right)\left(\frac{\frac{h}{t_0}\sum^{\frac{c\,t_0}{2\,\lambda_P}}\left(\frac{c\,t_0}{2\,(1+z+z_0)\lambda_P}\right)^n}{U(\lambda,T)\,4\pi^2c^2(1+z)^2}\right)^{1/3}. \quad (28)$$

Plots of the above equation for $0 \le z \le 20$ and $0 \le z \le z_s = 1090$ are presented in figures 3 and 4 respectively.

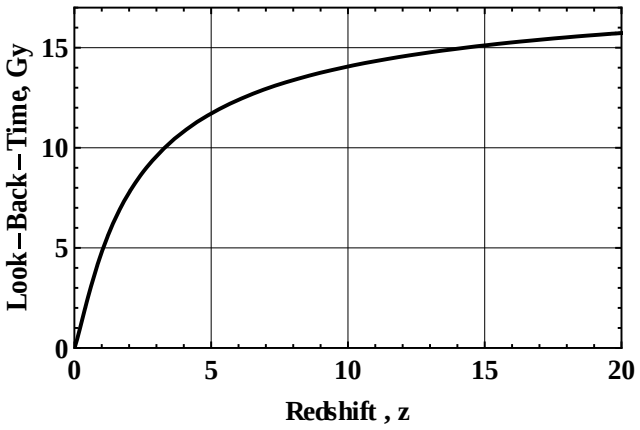

Figure 3. *Variations of the Look-Back-Time with Redshift for* $0 \le z \le 20$.

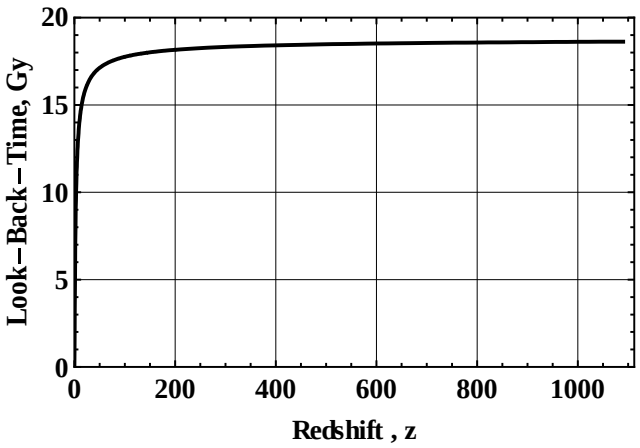

Figure 4. *Variations of the Look-Back-Time with Redshift for* $0 \le z \le z_s = 1090$.

Because the maximum age of the visible universe at the present time is about 14.9619 Gy, as figure 3 shows and equation (28) confirms, the maximum value that can be measured for the redshift is $z < 14.06$. Figure 4 shows that the maximum range of future visibility is up to $t_{cMax} = 18.850753$ Gy. This maximum corresponds to the redshift $z_s = z_{CMB} = 1090$ associated with the surface of last scattering. Therefore we conclude that t_{cMax} represents the future maximum range of visibility. That is, as the universe

ages further, one expects to be able to see objects up to 18.8953 billion light years away.

5. Predictions of the Model

In the following three sub-sections we present the details of the predictions of the distance redshift relation, the distance look-back-time relation, and the expansion velocity and the expansion acceleration with look-back-time.

5.1. Luminosity Distance Redshift Relation

In equation (28) the look-back-time, t_{LB}, represents the instantaneous temporal radius of the universe, with earth as its center. Considering the expansion of space and the relativity effect, using Lorentz transformation, it can be shown that the length of the luminosity time, t_L, is given by

$$t_L = \gamma t_{LB}. \tag{29}$$

Here γ is the Lorentz factor, which is given by

$$\gamma = \frac{1}{\sqrt{1-\left(\frac{u}{c}\right)^2}} = \frac{2+2\tilde{z}+\tilde{z}^2}{2(1+\tilde{z})} = \frac{2+2(z+z_0)+(z+z_0)^2}{2(1+(z+z_0))}. \tag{30}$$

In the above relation, u represents the Doppler redshift velocity, which is the relative velocity between the source and the observer, Harrison [27], and $\tilde{z} = z + z_0$ represents the redshift. Considering the "expanding balloon" model, as pointed out by Simionato, objects are points on the surface of the expanding balloon. Thus, based on equation (28), the luminosity distance, d_L, for any given value of the redshift, z, is given by

$$d_L = c\pi t_L = c\pi\gamma t_{LB} = c\pi\gamma\left[t_{cMax} - \frac{1}{Gy}\left(\frac{1+z_S}{2}\right)\left(\frac{\frac{h}{t_0}\sum^{\frac{c\,t_0}{2\,\lambda_P}}\frac{c\,t_0}{2\,(1+z+z_0)\,\lambda_P}^{n}}{U(\lambda,T)\,4\pi^2c^2(1+z)^2}\right)^{\frac{1}{3}}\right], \tag{31}$$

where $t_0 = 14.96185$ Gy, as given by equation (20), and $t_{cMax} = 18.8508$ Gy, as given by equation (27). The expanding balloon model implies that the universe has a positive curvature. This is consistent with Planck's CMB spectra which appear to be more consistent with the universe having a positive curvature, Di Valentino et al. [28].

To show the variations of the luminosity distance, d_L, with redshift, equation (31) is plotted in Figure 5. This figure appears to suggest that the luminosity distance is linearly proportional to the redshift. However, the slope of this curve, $\eta = \frac{ds(t_{LB})}{dz}$, is not constant, and it varies with the redshift.

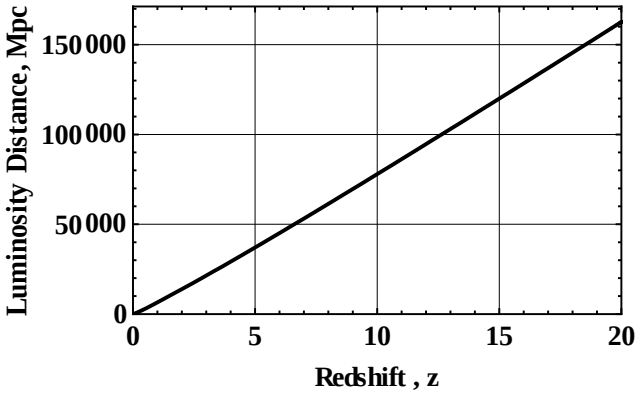

Figure 5. Variations of Luminosity Distance with Redshift.

5.2. Luminosity Distance Look-Back-Time Relation

Equations (28) and (31) relate the look-back-time and the luminosity distance to the redshift. For the same values of redshift, using these equations, we have tabulated the corresponding values for the look-back-time and the luminosity distance. To show the relation between the luminosity distance and the look-back-time, the corresponding tabulated values are used to plot Figure 6.

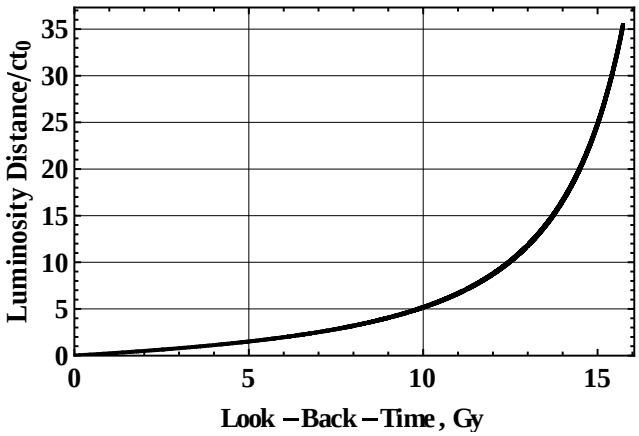

Figure 6. Variations of Luminosity Distance/ct_0 with Look-Back-Time.

5.3. Relations of the Expansion Velocity and Acceleration with Look-Back-Time

In order to evaluate the expansion velocity and the expansion acceleration, we first fit the following function,

$$\frac{d_L}{c\,t_0} = f(t_{LB}) = \sum_{i=1}^{i=12} a_i \left(e^{\left(\frac{t_{LB}}{16\,b_i}\right)^{1+i}} - 1\right), \tag{32}$$

to the data of figure 6 (values of a_i and b_i are given in the Appendix). For comparison purposes, the plot of equation

(32) is superimposed on the plot in figure 6 as shown in figure 7 (the Dashed Red Curve). Figure 7 confirms the fidelity of representation of the data of figure 6.

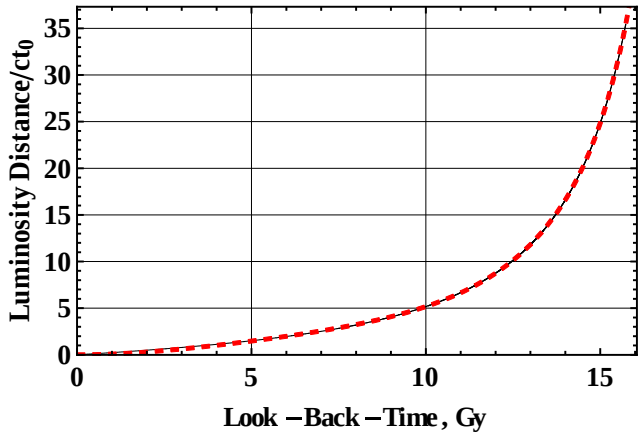

Figure 7. *Representation of Variations of Luminosity Distance/ct_0 with Look-Back-Time.*

The dimensionless expansion velocity, v_e/c, and the dimensionless expansion acceleration, a_e/g, are evaluated through differentiations with respect to the look-back-time, t_{LB}, that is

$$\frac{v_e}{c} = t_0 \frac{df(t_{LB})}{dt_{LB}}, \tag{33}$$

$$\frac{a_e}{g} = \frac{1}{g}\frac{d(v_e)}{dt_{LB}}, \tag{34}$$

where the gravitational acceleration on the earth surface, $g = 9.807\ m\ s^{-2}$, is used to make the expansion acceleration, a_e, dimensionless. Based on the above two equations, plots of variations of expansion velocity and expansion acceleration versus the look-back-time are presented in figures 8 and 9.

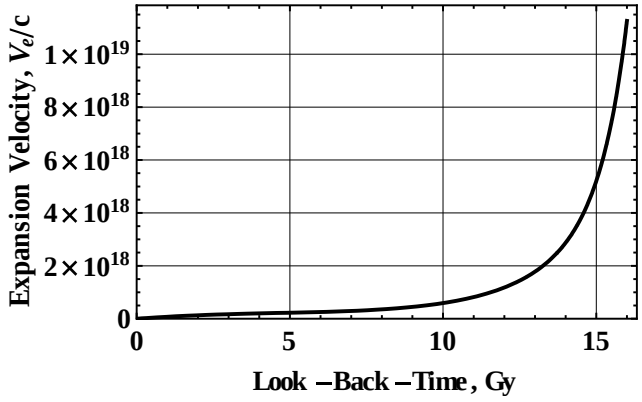

Figure 8. *Variations of Expansion Velocity with Look-Back-Time.*

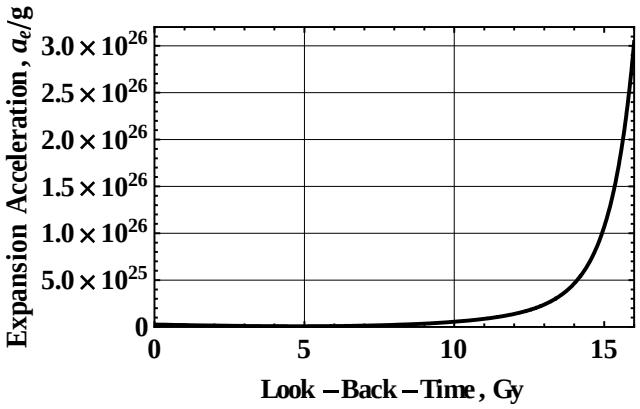

Figure 9. *Variations of Expansion Acceleration with Look-Back-Time.*

To better display the more recent variations of expansion velocity and expansion acceleration, equations (33) and (34) are replotted in figures 10 and 11 for $0 < t_{LB} \leq 9$ Gy. Figure 10 shows an inflection point in the velocity at $t_{LB} \cong 5$ Gy, and figures 11 and 12 confirm that the location of the inflection point is at $t_{LB} \approx 4.77$ Gy. Looking forward from CMB emission toward the present time, as seen from figure 10, the expansion decelerates all the way toward the present time. The expansion velocity decelerates at reducing rates till the inflection point. After the inflection point, the expansion velocity decelerates at increasing rates toward the present time. Looking back in time, figure 11 shows that the expansion acceleration is always positive. To better characterize the expansion acceleration, its rate of change, jerk $= \frac{d(a_e)}{dt_{LB}}$, is plotted in figure 12. This figure shows that the jerk is initially negative but it crosses the zero at $t_{LB} \approx 4.77$ Gy, after which it remains positive.

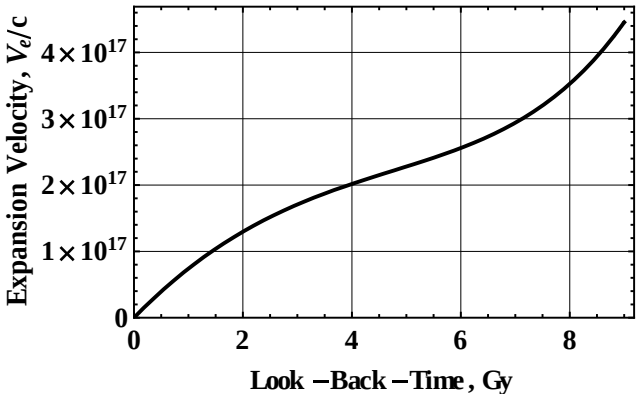

Figure 10. *Representation of Variations of Expansion Velocity with Look-Back-Time.*

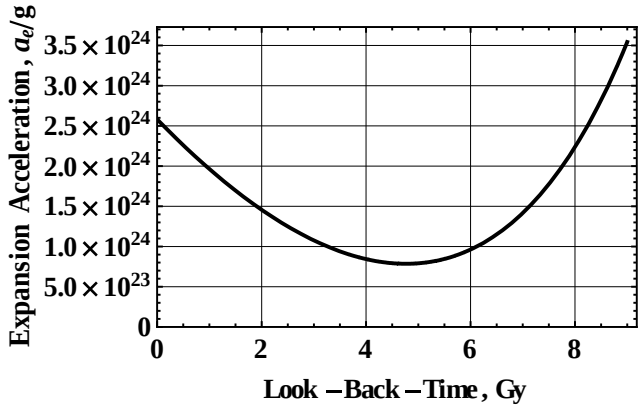

Figure 11. *Representation of Variations of Expansion Acceleration with Look-Back-Time.*

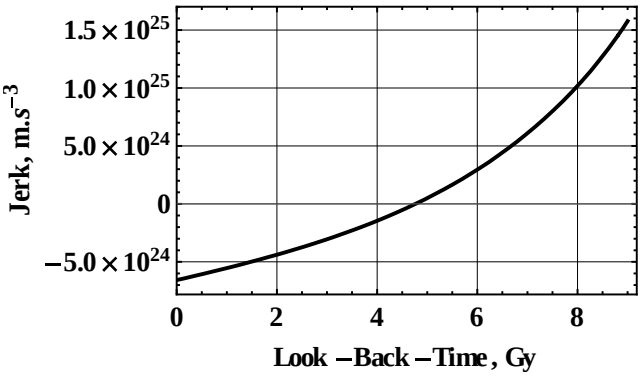

Figure 12. *Variations of Rate of Change of Expansion Acceleration with Look-Back-Time.*

6. Evaluation of Energy Density

Based on equations (6), (13) and (21), the output gy, E_1, and the input energy, E_2, are given as follows:

$$E_1 = U(\lambda, T)\,(4\pi\, r_s{}^2)\,\pi\, t_{CMB} = U(\lambda, T)\,4\pi^2 c^2 (1 + z_s)^2\,(410829\ y)^3 = 1.34552\times10^{70}\ j. \quad (35)$$

$$E_2 = \frac{h}{t_{obs}} \sum_{n_o}^{n_e} n = \frac{h}{t_{obs}} \sum_{\frac{c\,t_{obs}}{2\,(1+z_S)\,\lambda_P}}^{\frac{c\,t_{obs}}{2\,\lambda_P}} n = \frac{h}{t_0} \sum_{\frac{c\,t_0}{2\,(1+z_S)\,\lambda_P}}^{\frac{c\,t_0}{2\,\lambda_P}} n = 1.34552\times10^{70}\ j. \quad (36)$$

As expected, the input and output energies, E_1 and E_2, are equal to each other. Using equation (35) we see that the energy density per square area, ρ_A, is constant, and its value is given by

$$\rho_A = \frac{E_1}{A} = \frac{E_1}{4\pi\, r_s{}^2} = U(\lambda, T)\,\pi\, t_{CMB} = 1.462\times10^6 \times \pi \times 410829\ y = 5.95471\times10^{19}\ j.m^{-2}. \quad (37)$$

This constant surface energy density provides the pressure that is perpetuating the expansion of the universe. As seen from equation (37), this energy density is independent of time, and its value does not change no matter how much the universe expands. The source of this constant surface energy density is the momentum energy of photons. Photons have no mass; and as seen from equations (35) and (36), the constant surface energy density, ρ_A, involves no mass.

The energy density per unit volume is given by

$$\rho = \frac{E_2}{A} = \frac{E_1}{A} = \frac{E_1}{\frac{4\pi}{3} r_s{}^3} = \frac{4\pi\, r_s{}^2 \rho_A}{\frac{4\pi}{3} r_s{}^3} = \frac{3\,\rho_A}{r_s} = \frac{P}{w}, \quad (38)$$

where ρ represents energy per unit volume, P represents pressure, and $w = p/\rho$ is the "equation of state." Thus

$$w = \frac{P}{\rho} = \frac{1}{3}\frac{P\, r_s}{\rho_A}. \quad (39)$$

Since the input energy, E_2, is equal to the output energy, E_1, the work down by the pressure going through the distance, r_s, generates the input energy per unit area that must be equal to the output energy per unit area, ρ_A. That is, $P\, r_s = \rho_A$. Thus substitution for $P\, r_s$ back into equation (39) yields

$$w = \frac{P}{\rho} = \frac{1}{3}, \quad (40)$$

which represents the "equation of state" for relativistic radiations that in our case are the released photons. It should be noted that the above result is consistent with a spherically expanding universe. Therefore, the path of photons, from the surface of last scattering to the present time, must be along the arc of a curve on the periphery of the expanding universe. This is in agreement with General Relativity, according to which light follows the curvature of space time.

7. Check of Consistency of the Predictions of the Model with the Observational Data

7.1. Consistency of Ages of the Four JWST Spectroscopically Confirmed High Redshift Galaxies

The names of these four galaxies and their corresponding spectroscopically measured redshifts, as reported by Curtis-Lake, et al. are listed in Table 1. Considering the present age of the universe to be $t_0 = 14.9618$ Gy, as given by the proposed model, and the corresponding measured redshift, the ages of these galaxies are evaluated via the look-back-time, t_{LB}, given by equation (28). These ages are listed in the third column of Table 1. The ages of these galaxies are also calculated using UCLA Cosmological Calculator (astro.ucla.edu), with 2018 ΛCDM parameters' values: $H_0 = 67.4$ and $\Omega_m = 0$, and the present-time age of the visible

universe, $\tilde{t}_0 = 13.791$ Gy. These ages are listed in the fourth column of Table 1. For comparison we modify the ages in the fourth column by multiplying them by the ratio $\frac{t_0}{\tilde{t}_0} = 14.962/13.791$ and listing the results in the fifth column of this table. The last column of this table shows the percent difference between the ages of galaxies, given in the third column, and the ages calculated based on the ΛCDM model listed in the fifth column. These small differences demonstrate the consistency of the predictions of the ages of galaxies via the proposed model with the ΛCDM model predictions. As a further demonstration of the utility of the model, the ages of galaxies, as listed in the third column of table 1, are plotted on the plot of figure 3 in figure 13.

Table 1. *Spectroscopic Redshifts and Ages of Galaxies.*

Name JADES	Spectroscopic Redshift, z	Age, Gy $t_0 = 14.962$ Gy	Age, Gy $\tilde{t}_0 = 13.791$ Gy	Age, Gy Modified Age	Percent Difference
GS-z13-0	$13.20^{+0.04}_{-0.07}$	14.8069	13.471	14.615	1.2968
GS-z12-0	$12.63^{+0.24}_{-0.08}$	14.6954	13.451	14.593	0.6908
GS-z11-0	$11.58^{+0.05}_{-0.05}$	14.4686	13.407	14.545	-0.5310
GS-z10-0	$10.38^{+0.07}_{-0.06}$	14.1677	13.345	14.478	-2.1914

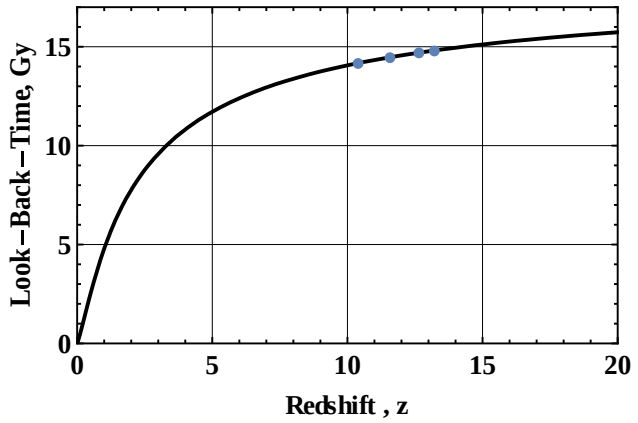

Figure 13. *Prediction of Galaxies Ages via the Look-Back-Time Redshift Relation.*

7.2. Comparisons of Distance Moduli with Observational Data

To check the consistency with observational data we first evaluate the distance modulus, μ, based on the luminosity distance, d_L, as given by equation (31). The distance modulus is defined by

$$\mu = 25 + 5\,\text{Log}\,\frac{d_L}{\text{Megaparsec}}. \quad (41)$$

Equation (41) is plotted in figures 14 and 15 for the values of redshift $0 \le z \le 20$. To check how well the curve in these figures represents the observational data, the following sets of observational data are also plotted in these figures:

1. A set of 557 SNe data with redshifts from a low of $z = 0.0152$ to a maximum of $z = 1.4$, as reported in the Union2 Compilation [29]. In figures 14 and 15 these data points are shown in red.
2. A set of 394 extragalactic distances to 349 galaxies with cosmological redshifts from a low of $z = 0.133$ to a maximum of $z = 6.6$, as reported by Mador and Steer [30]. In figures 14 and 15 these data points are shown in blue.
3. A set of the 4 most distant astronomical objects observed by JWST with spectroscopically determined redshifts. These redshifts are from $z = 10.38$ to a maximum of $z = 13.20$, as listed in Table 1. For these galaxies the distance moduli are calculated based on the modified ages as listed in the fifth column of Table 1. The distance moduli for these galaxies are also plotted in figures 14 and 15. The data points corresponding to these distances are shown in black.

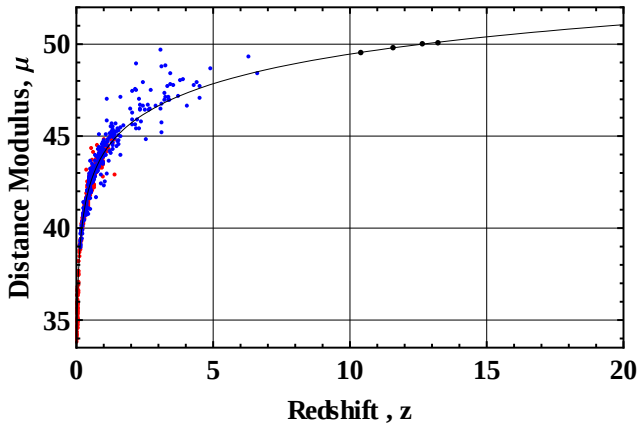

Figure 14. *Comparison of the Prediction of the Present Model with Observational Data.*

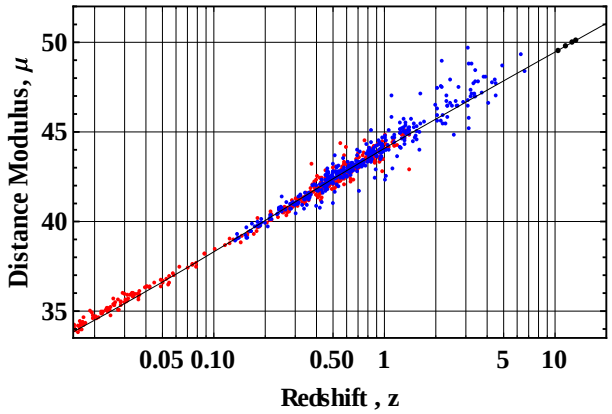

Figure 15. *Comparison of the Prediction of the Present Model with Observational Data.*

8. Evaluation of the Hubble Constant and the Cause of Tension in the Measurements

The proposed model is totally independent of the ΛCDM model. It involves neither its Hubble constant nor its dark matter/energy or any cosmological constant. There is no derived parameter in this model; the only input to the model is the redshift, whether measured or assumed. In this section it is shown how this analytical model can be used to calculate the Hubble constant, H_0.

The present time age of the visible universe, as given by equation (20), is $t_0 = 14.96185$ Gy. At the present time the closest we can get to the instant of the big bang, as given by equation (26), is $\Delta t_c = 0.224107$ Gy. Thus the maximum length of the look-back-time at the present is given by

$$t_s = t_0 - \Delta t_c \tag{42}$$

But because the expansion is isotropic, the length of time between the surface of last scattering and the present time is given by

$$t_{H_0} = 2t_s - t_0 = 2\,(t_0 - \Delta t_c) - t_0 = t_0 - 2\,\Delta t_c = 14.5136 \text{ Gy} \tag{43}$$

The time t_{H_0} above represents the Hubble time, which yields the following value for the Hubble constant:

$$H_0 = \frac{1}{t_{H_0}}\frac{\text{Mpc}}{1000} = \frac{1}{14.5136 \text{ Gy}}\frac{\text{Mpc}}{1000} = 67.3383 \text{ km s}^{-1}\text{ Mpc}^{-1} \tag{44}$$

This is almost identical to the value of $H_0 = 67.4 \pm 0.5$ km s^{-1}Mpc^{-1} as reported by Planck observations.

8.1. A Discovery

It should also be mentioned that during this work we discovered that the naturally constant number $\pi^2 \frac{G}{c}\frac{1\text{ kg}}{1\text{ m}^2}\frac{\text{Mpc}}{1000} = 67.7661$ km s^{-1} Mpc^{-1} happens to be consistent with the Planck observations reported value of $H_0 = 67.4 \pm 0.5$ km s^{-1} Mpc^{-1}. However, if this number is considered to be the correct value of H_0, then according to the proposed model, assuming the present time temperature of the universe is $T_0 = 2.752799$ K, a temperature of $T_s = 3226.395$ K at the CMB emission would increase the redshift at the CMB emission to $z_s = \frac{T_s}{T_0} = \frac{3226.395}{2.752799} = 1172.0418$ K. Substitutions of $T_s = 3226.395$ K and $z_s = 1172.0418$ in the proposed model will yield the age of the visible universe as $t_0 = 14.422010$ Gy, $t_{CMB} = 350929.607008$ y, and $\Delta t_c = 0.205827$ Gy. Using these values for t_0 and Δt_c, the model yields the Hubble time $t_{H_0} = 14.010355$ Gy and the Hubble constant $H_0 = 67.7661$ km s^{-1} Mpc^{-1}. This value for H_0 matches the constant number $\pi^2 \frac{G}{c}\frac{1\text{ kg}}{1\text{ m}^2}\frac{\text{Mpc}}{1000}$ exactly.

8.2. The Cause of Tension in the Measurements of the Hubble Constant

The two well known sets of measurements of H_0 that are in tension with each other are:
one by Reiss et al., which reports a value of

$$H_{0_R} = 73.2 \pm 1.3 \text{ km s}^{-1}\text{ Mpc}^{-1}, \tag{45}$$

and the other by the Planck Collaboration, which reports a value of

$$H_{0_P} = 67.4 \pm 0.5 \text{ km s}^{-1}\text{Mpc}^{-1}. \tag{46}$$

To explain the cause of tension between the H_{0_R} value and H_{0_P} value, we first derive their values using the proposed model.

(**A**). To derive H_{0_R} we assume the present age of the visible universe, as assumed by Reiss et al., is

$$t_{0_R} = 13.791 \text{ Gy}. \tag{47}$$

Substitution of this age into equation (21) yields the age of the universe at CMB emission as

$$t_{CMB_R} = \frac{1}{y}\left(\frac{\frac{h}{t_{0_R}}\sum^{n}\frac{c\,t_{0_R}}{2\,\lambda_P}}{U(\lambda,T)\,4\pi^2c^2(1+z_s)^2}\right)^{1/3} = 399819.680433 \text{ y}. \tag{48}$$

Therefore, according to equation (26), the temporal radius of the surface of last scattering, Δt_{c_R}, at the assumed present time, t_{0_R}, is given as

$$\Delta t_{c_R} = \frac{1+z_s}{2}\, t_{CMB_R} = \left(\frac{1+z_s}{2}\right)\frac{1}{y}\left(\frac{\frac{h}{t_{0_R}}\sum^{n}\frac{c\,t_{0_R}}{2\lambda_P}}{\frac{U(\lambda,T)\,4\pi^2c^2(1+z_s)^2}{2\,(1+z_s)\,\lambda_P}}\right)^{1/3} = \frac{1+1090}{2}\,\frac{399819.680433\ y}{Gy} = 0.218102\ Gy. \quad (49)$$

Thus the Reiss et al. Hubble time, $T_{H_{0_R}}$, based on the model, is given by

$$T_{H_{0_R}} = t_{0_R} - 2\,\Delta t_{c_R} = 13.791\ Gy - 2(0.218102\ Gy) = 13.3548\ Gy. \quad (50)$$

This Hubble time yields the value for the Hubble constant as

$$H_{0_R} = \frac{1}{T_{H_{0_R}}}\frac{Mpc}{1000} = \frac{1}{13.3548\ Gy}\,\frac{Mpc}{1000} = 73.1815\ km\ s^{-1}\ Mpc^{-1} \quad (51)$$

This value of the Hubble constant is essentially identical with the measured value of $73.2 \pm 1.3\ km\ s^{-1}Mpc^{-1}$ as reported by Reiss et al.

(B). The Planck Collaboration Hubble constant given in equation (46) yields its associated Hubble time as

$$T_{H_{0_P}} = \frac{1}{H_{0_P}}\frac{Mpc}{1000} = \frac{1}{67.4}\,\frac{Mpc}{1000\ Gy}\,\frac{1}{Gy} = 14.5003\ Gy. \quad (52)$$

The Planck Collaboration age of the universe, t_{0_P}, is given by

$$t_{0_P} = T_{H_{0_P}} + 2\,\Delta t_{c_p}. \quad (53)$$

Initially Δt_{c_p} is assumed to be equal to $\Delta t_c = 0.224107\ Gy$ given by equation (26). Substitution of this value of Δt_c into equation (53) yields $t_{0_P} = 14.948562\ Gy$. Substitution of this value of t_{0_P} in place of t_0 into equation (26) yields the temporal radius of the surface of last scattering at the present time as

$$\Delta t_{c_p} = \frac{1+z_s}{2}\, t_{CMB_P} = \frac{1+z_s}{2}\,\frac{1}{y}\left(\frac{\frac{h}{t_{0_P}}\sum^{n}\frac{c\,t_{0_P}}{2\lambda_P}}{\frac{U(\lambda,T)\,4\pi^2c^2(1+z_s)^2}{2\,(1+z_s)\,\lambda_P}}\right)^{1/3} = 0.224041\ Gy. \quad (54)$$

Substituting this value of Δt_{c_p} back into equation (53) and repeating this cyclical process, after six cycles we find $\Delta t_{c_p} = 0.2240399\ Gy$. The seventh cycle gives the same value. Thus, based on the model, the Planck Collaboration age of the universe at the present time, t_{0_P}, is given by

$$t_{0_P} = T_{H_{0_P}} + 2\,\Delta t_{c_p} = 14.5003\ Gy + 2 \times 0.2240399\ Gy = 14.9484\ Gy. \quad (55)$$

Substitution of this age into equation (21) yields the age of the universe at CMB emission as

$$t_{CMB_P} = \frac{1}{y}\left(\frac{\frac{h}{t_{0_P}}\sum^{n}\frac{c\,t_{0_P}}{2\lambda_P}}{\frac{U(\lambda,T)\,4\pi^2c^2(1+z_s)^2}{2\,(1+z_s)\,\lambda_P}}\right)^{1/3} = 410{,}706.950027\ y. \quad (56)$$

Therefore the temporal radius of the surface of last scattering at the time t_{0_P} is given by

$$\Delta t_{c_P} = \frac{1+z_s}{2}\, t_{CMB_P} = \frac{1+1090}{2}\,\frac{410706.950027\ y}{Gy} = 0.224107\ Gy. \quad (57)$$

Thus the Hubble time, $T_{H_{0_P}}$, is given by

$$T_{H_{0_P}} = t_{0_P} - 2\,\Delta t_{c_P} = 14.9486\ Gy - 2\ (0.224107\ Gy) = 14.5003\ Gy. \quad (58)$$

This Hubble time yields the value for the Hubble constant as

$$H_{0_P} = \frac{1}{T_{H_{0_P}}}\frac{Mpc}{1000} = \frac{1}{14.5003\ Gy}\,\frac{Mpc}{1000} = 67.4\ km\ s^{-1}\ Mpc^{-1}. \quad (59)$$

This calculated value of H_{0_P} exactly matches the reported value of $H_{0P} = 67.4 \pm 0.5\ km\ s^{-1}Mpc^{-1}$ given in equation (46). It differs from the value $H_0 = 67.3383\ km\ s^{-1}\ Mpc^{-1}$ given by the proposed model by less than 0.092%.

Assuming the present time age of the visible universe to be $t_0 = 13.791\ Gy$, the proposed model predicted the value, as given by equation (51), of $H_{0_R} = 73.1815\ km\ s^{-1}\ Mpc^{-1}$, which differs from the value $H_{0_R} = 73.2\ km\ s^{-1}\ Mpc^{-1}$ by less than 0.026%. Also the proposed model prediction of the age of the visible universe of $t_0 = 14.96185\ Gy$ is very close to the age of $t_{0_P} = 14.9484\ Gy$, calculated based on the Planck Collaboration measurement, differing from it by less than 0.089. Thus it can be concluded that the predictions of the model for H_{0_R} and H_{0_P} are consistent with their corresponding value as measured by the Reiss et al. and as measured by the Planck Collaboration.

Comparing equation (47) with equation (55), it is seen that the age of the universe, t_{0_P} according to the Planck Collaboration, is greater than the age of the universe, t_{0_R} according to the Reiss et al. This difference in the age of the universe gives rise to the tension between H_{0_R} and H_{0_P}. The Planck Collaboration measurement, using CMB temperature fluctuations power spectra, is non-local: its starting point is close to the surface of last scattering. The path of light for the evaluation of the luminosity distance, according to the

model, is along a curve on the periphery of the expanding universe. According to the proposed model, the Planck Collaboration measurement can effectively be considered to be along a curve. This is in agreement with General Relativity, according to which light follows the curvature of space time.

But the Reiss et al. measurement, starting from the earth using the cosmic distance ladder, measures the straight line time distance along the chord of a curve which is the same curve along whose arc the Planck Collaboration measurement has effectively been performed.

8.3. Confirmation of the Cause of Tension in the Measurements of the Hubble Constant

As a proof of the cause of tension we consider equations (50) and (52) or equivalently equations (45) and (46). Based on these equations, the ratio of the Planck Collaboration and the Reiss et al. Hubble times is given as

$$\frac{T_{H_{0P}}}{T_{H_{0R}}} = \frac{H_{0R}}{H_{0P}} = \frac{14.5003\ \text{Gy}}{13.3548\ \text{Gy}} = 1.085774. \quad (60)$$

The ratio of the Arc length to the Chord length for a circular arc subtending the angle $\theta = 1.393768$ radians is given by the following relation:

$$\frac{\text{Arc Length}}{\text{Chord Length}} = \frac{\theta/2}{\text{Sin}\{\theta/2]} = \frac{0.696884}{\text{Sin}\{0.696884\}} = 1.085774. \quad (61)$$

The identical results from the above two equations reveal the cause of the tension: one evaluates the length of time along a curve, while the other evaluates the length of time along the chord of the same curve.

Further in the following we show that the left-over part, angle ϕ, accounts for the reductions of $2\,\Delta t_{c_R}$ and $2\,\Delta t_{c_P}$ in equations (50) and (58) respectively. The left over angle ϕ is given by

$$\phi = \frac{\pi}{2} - \theta = \frac{\pi}{2} - 1.393768 = 0.177028\ \text{radian}. \quad (62)$$

The ratio of the arc length to the chord length for angle ϕ is given by

$$\frac{\phi}{\text{Sin}\{\phi]} = \frac{0.177028}{\text{Sin}\{0.177028\}} = 1.005242. \quad (63)$$

Using the values for Δt_{c_R} and Δt_{c_P}, as given in equations (49) and (54), their ratio is given by the following relation:

$$\frac{2\,\Delta t_{c_P}}{2\,\Delta t_{c_R}} = \frac{0.224041\ \text{Gy}}{0.218102\ \text{Gy}} = 1.02723. \quad (64)$$

The difference between above two ratios is less than 2.2% and this is within the stated errors associated with the two measured values of H_0. This result provides further confirmation that the Planck Collaboration measurement is along a circular arc, while the Reiss et al. measurement is along the chord of the same circular arc.

9. Summary and Conclusions

In this work, we have formulated an analytical model that involves neither the Hubble constant nor any dark matter/energy. The only input to the model is the measured or assumed redshift. Based on a temperature of about 3000 K and the redshift $z_{CMB} = 1090$, associated with the surface of last scattering, the model makes the following predictions:

1) The present time age of the visible universe is $t_0 = 14.96185$ Gy.
2) The age of the universe when the electromagnetic waves start to be emitted is $t_{emi} = 50,280.1$ y.
3) The age of the universe at CMB emission, $t_{CMB} = 410,829$ y.
4) The ultimate range of visibility for the observable universe is $t_{0c} = 18.8508$ Gy.
5) The relation between the look-back-time and redshift.
6) The relation between luminosity distance and redshift.
7) The relation between luminosity distance and look-back-time.
8) The relations between the expansion velocity and the look-back-time, and between the expansion acceleration and the look-back-time.
9) The expansion of the universe is perpetuated by the constant surface energy density, $\rho_A = 5.9407 \times 10^{19}$ j. m^{-2}.
10) The Hubble constant is equal to $H_0 = 67.3383$ km s^{-1} Mpc^{-1}.
11) If one assumes the temperature at CMB emission to have been $T_s = 3226.395$ K rather than 3000 K, then the Hubble constant would be equal to $H_0 = \pi^2 \frac{G}{c} \times \frac{1\ \text{kg}}{1\ \text{m}^2} \times \frac{\text{Mpc}}{1000} = 67.7661$ km s^{-1} Mpc^{-1}.

The comparisons with observational data demonstrate consistency of the predictions of this model with observational data as well as with both the Reiss et al. and the Planck measurements. The model also shows that the cause of the tension in the measurements of the Hubble constant is due to the different paths along which the measurements are effectively performed.

Abbreviations

CMB	Cosmic Microwave Background
CDM	Cold Dark Matter

Acknowledgments

All the numerical work and plots are done via Wolfram Mathematica v.10.0, 4/3/2014.

Author Contributions

Naser Mostaghel is the sole author. The author read and approved the final manuscript.

Data Availability Statement

The distance moduli redshift data are available at:
http://ned.ipac.caltech.edu/level5/NED4D/
https://supernova.lbl.gov/Union/figures/SCPUnion2_mu_vs_z.txt

Conflicts of Interest

The author declares no conflicts of interest.

Appendix

$a_1 = 5.608219$ $b_1 = 0.699974$
$a_2 = -9.847286$ $b_2 = 0.853344$
$a_3 = -2.725458$ $b_3 = 0.895378$
$a_4 = 4.921901$ $b_4 = 0.994736$
$a_5 = 12.128504$ $b_5 = 0.980083$
$a_6 = 5.660950$ $b_6 = 0.994855$
$a_7 = 3.727886$ $b_7 = 0.968882$
$a_8 = 3.218413$ $b_8 = 1.186152$
$a_9 = 1.887220$ $b_9 = 1.170088$
$a_{10} = -0.645297$ $b_{10} = 1.0526943$
$a_{11} = 5.608219$ $b_{11} = 0.699974$
$a_{12} = -9.847286$ $b_{12} = 0.853344$

References

[1] Riess, A. G., Casertano, S., Yuan, W., et al., (2021), "Cosmic Distances Calibrated to 1% Precision with Gaia EDR3 Parallaxes and Hubble Space Telescope Photometry of 75 Milky Way Cepheids Confirm Tension with ΛCDM," Apj, 908, L6.

[2] Aghanim, N., Akrami, Y., Ashdown, M., et al., (2021), "Planck 2018 Results. VI. Cosmological Parameters," Astronomy & Astrophysics, 571, A6, arXiv: 2208.07467v1, Aug 2021.

[3] Di Valentino, E., 2021, "In the Realm of the Hubble Tension – a Review of Solutions," Preprint, arXiv: 2103.01183v3.

[4] Di Valentino, E., 2021, "A Combined Analysis of the H_0 Late Time Direct Measurements and the Impact on the Dark Energy Sector," Royal Astronomical Society, 502, 2065-2073.

[5] Abbott, T. M. C., Abdalla, J., Annis, K., et al., 2018, "Dark Energy Survey Year 1 Results: A Precise H_0 Measurement from DES Y1, BAO, and D/H Data," Preprint, arXiv: 1711.00403v1.

[6] Schombert, J., McGaugh, S., Lelli, F., "Using the Baryonic Tully–Fisher Relation to Measure Ho," 2020, AJ, 160, 71.

[7] Freedman, W. A, Madore, B. F., Taylor Hoyt, et al.., (2020), "Calibration of the Tip of the Red Giant Branch," ApJ, 891, 57.

[8] Huang, C. D., Reiss, A. G., et al., 2020, "Hubble Space Telescope Observations of Mira Variables in the SN Ia Host NGC 1559: An Alternative Candle to Measure the Hubble Constant," Apj, 889, 5.

[9] Bull, P., Akrami, Y., et al., 2016, "Beyond Lamda CDM: Problems, Solutions, and the Road Ahead," https://arXiv.org/abs/1512.05356

[10] Boylan-Kolchin, M., Weisz, D. R., (2021), "Uncertain Times: the Redshift-time relation from Cosmology and Stars," Royal Astronomical Society, 505, 2764-2783.

[11] Jakobsen, P., Ferruit, C., Alves de Oliveira, S., et al., 2022, "The Near-Infrared Spectrograph (NIRSpec) on the James Webb Space Telescope. I. Overview of the instrument and its capabilities," Astronomy & Astrophysics, 661, A80.

[12] Roszkowski, L., Sessolo, E. M., Trojanowski, S., 2018, "WIMP dark matter candidates and searches—current status and future prospects," 2018 Rep. Prog. Phys. 81, 066201.

[13] Schlaufman, K. C., Thompson, I. B., Casey, A. R., 2018, "An Ultra Metal-poor Star Near the Hydrogen-burning Limit," ApJ, 867, 98.

[14] Hill, V., Christlieb, N., Beers, T. C., et al., 2017, "The Hamburg/ESO R-process Enhanced Star survey (HERES) XI. The highly r-process-enhanced star CS 29497-004," A & A, 607, A91.

[15] Abdalla, E, Abellan, G. F., Aboubrahim, A., et al., 2022, "Cosmology Intertwined: A Review of the Particle Physics, Astrophysics, and Cosmology Associated with the Cosmological Tensions and Anomalies," Preprint, arXiv: 2203.06142v3, 2022.

[16] Greene, B., Perlmutter, S., 2022, Jan 6, World Science Festival, YouTube, https://www.youtube.com/watch?v=zokNLqGd9TQ

[17] Freedman, L. F., (2017), "Cosmology at Crossroads: Tension with the Hubble Constant," Nature Astronomy, 1, 0169 (2017).

[18] Pasten, E., Cardenas, V. H., 2023, "Testing ΛCDM Cosmology in a Binned Universe: Anomalies in the Deceleration Parameter," Preprint, arXiv: 2301.10740v1.

[19] Robertson, B. E., Tacchella, S., Johnson, B. D., et al., 2022, "Discovery and properties of the earliest galaxies with confirmed distances," Preprint, arXiv 2212.04480.

[20] Curtis-Lake, E., Carniani, S., Cameron, A., 2022, "Spectroscopy of four metal-poor galaxies beyond redshift ten," Preprint, arXiv: 2212.04568v1.

[21] Brinchmann, J., 2022, 'High-z galaxies with JWST and local analogues—it is not only star formation," MNRAS 000, 1-19 (2022).

[22] Goldin, E., (1982), "Waves and Photons, An Introduction to Quantum Optics," John Wiley & Sons, New York.

[23] Kramm, G., Molders, N., (2009), "Planck's Blackbody Radiation Law," Preprint, arXiv: 0901.1863v2, !@ Nov 2009.

[24] Simionato, Silvia, 2021, "Three Redshifts: Doppler, Cosmological, and Gravitational," The Physics Teacher, Vol. 59, May 2021.

[25] Fixsen, D. J., 2009, "The Temperature of the Cosmic Microwave Background," The Astrophysical Journal. 707 (2): 916-920. arXiv: 0911.1955 (astro-ph.CO) 10. Nov 2009.

[26] Schwarzschild, B. 2005, Physics Today, 58, March, 19-21.

[27] Harrison, E., 1993, "The Redshift-Distance and Velocity-Distance Law," ApJ, 403: 28-31.

[28] Di Valentino, E., Melchiorri, A., Silk, J., 2020, "Planck Evidence for a Closed Universe and a Possible Crisis for Cosmology," Nature Astronomy 4, 196-203.

[29] Amanullah, R., Lidman, C., Rubin, D., et al. 2010, "Spectra and Hubble Space Telescope Light Curves of Six Type Ia Supernovae at 0.511 <z< 1.12 and the Union2 Compilation," Apj, 716: 712-738
https://supernova.lbl.gov/Union/figures/SCPUnion2_mu_vs_z.txt

[30] Madore, B. F., Steer, I. P., 2008, "NASA/IPAC, Extragalactic Distances Database Master List of Galaxy Distances," NED-4D, http://ned.ipac.caltech.edu/level5/NED4D/